Available online at www.sciencedirect.com
ScienceDirect
Journal of the European Ceramic Society 28 (2008) 2717–2724
www.elsevier.com/locate/jeurceramsoc

Synthesis of lanthanum silicate oxyapatite materials as a solid oxide fuel cell electrolyte

Emilie Béchade [a], Isabelle Julien [a], Tomoyuki Iwata [b], Olivier Masson [a], Philippe Thomas [a], Eric Champion [a,*], Koichiro Fukuda [b]

[a] *Sciences des Procédés Céramiques et de Traitements de Surface (SPCTS), UMR 6638 CNRS, Faculté des Sciences et Techniques, Université de Limoges, 123 Avenue Albert Thomas, 87060 Limoges Cedex, France*

[b] *Department of Environmental and Materials Engineering, Nagoya Institute of Technology, Nagoya 466-8555, Japan*

Received 19 September 2007; received in revised form 12 March 2008; accepted 20 March 2008
Available online 22 May 2008

Abstract

Lanthanum silicate oxyapatites of structural formula $La_{9.33+x}(SiO_4)_6O_{2+1.5x}$ ($0 < x < 0.27$) are currently investigated for their high ionic conductivity. We have studied the synthesis of pure apatite powders, especially $La_{9.33}(SiO_4)_6O_2$ and $La_{9.56}(SiO_4)_6O_{2.34}$, by solid state reactions. We have finalized a synthesis process which limits the formation of the often encountered secondary phases La_2SiO_5 and $La_2Si_2O_7$ by using an appropriate thermal treatment of the starting mixture. Lanthanum oxyapatite powders were synthesized at a temperature much lower (1200 °C) than that used in the conventional powder solid-state synthesis routes ($T > 1600$ °C). X-ray diffraction, scanning electron microscopy and specific surface area measurements were used to analyze the structural and microstructural changes of the as prepared powders heated at different temperatures. Electrical characterization of pure sintered materials was conducted and showed that the incorporation of extra oxide ions, corresponding to the $La_{9.56}(SiO_4)_6O_{2.34}$ composition, enhanced the ionic conductivity by one order of magnitude when comparing to that of the $La_{9.33}(SiO_4)_6O_2$ sample.
© 2008 Elsevier Ltd. All rights reserved.

Keywords: Powders-solid state reaction; Ionic conductivity; Apatite; Fuel cells $La_{9.33}(SiO_4)_6O_2$

1. Introduction

Oxide ion conductors working at moderate temperatures have a huge market potential as electrolytes for solid oxide fuel cells (SOFCs). The direct conversion of chemical to electrical energy through an electrochemical reaction is allowed by this device with excellent environmental compatibilities. However, the widely used yttria stabilized zirconia (YSZ) works as electrolyte only at high temperatures (900–1000 °C). To overcome disadvantages of these high operating temperatures, other oxide ion conductors working at intermediate temperatures (600–800 °C) are actively investigated to replace YSZ.[1] Recently, significant researches have been performed on lanthanum silicates with an apatite-type structure with composition $La_{9.33}(SiO_4)_6O_2$ which exhibits high ionic conductivity at lower temperatures ($\sigma = 7.2 \times 10^{-5}$ S cm^{-1} at 500 °C and 1.4×10^{-3} S cm^{-1} at 800 °C).[2] Electrical properties could be enhanced by the incorporation of excess La_2O_3 into this structure[3–5] in order to form hypothetical $La_{9.33+x}(SiO_4)_6O_{2+1.5x}$ ($x > 0$) compositions. It is achieved by filling interstitial sites with oxide ions located near the 2a sites (0, 0, 0.25) of the $P6_3/m$ unit cell (Fig. 1). For these compositions, either La_2SiO_5 or $La_2Si_2O_7$ are easily formed as secondary phases. Once they appear, it is very difficult to eliminate them by further firing.

Studies performed on the synthesis of apatite-type lanthanum silicates by solid state reactions have indicated that repeated long thermal treatments at high temperatures are required to prepare pure apatite-type lanthanum silicate when starting from La_2O_3 and SiO_2.[4,6–9] These high temperatures present some disadvantages such as a poor control of the morphology and particle size. To overcome these problems, other methods have been developed such as mechanochemical synthesis and sol–gel route.[2,10–12] However, the sol–gel route implies several heating steps to promote the formation of a gel and ensure the removal of all the organic components. Mechanochemical synthesis needs a long milling time (higher than 9 h) of the starting mixture.

* Corresponding author. Tel.: +33 555457460; fax: +33 555457586.
E-mail address: eric.champion@unilim.fr (E. Champion).

0955-2219/$ – see front matter © 2008 Elsevier Ltd. All rights reserved.
doi:10.1016/j.jeurceramsoc.2008.03.045

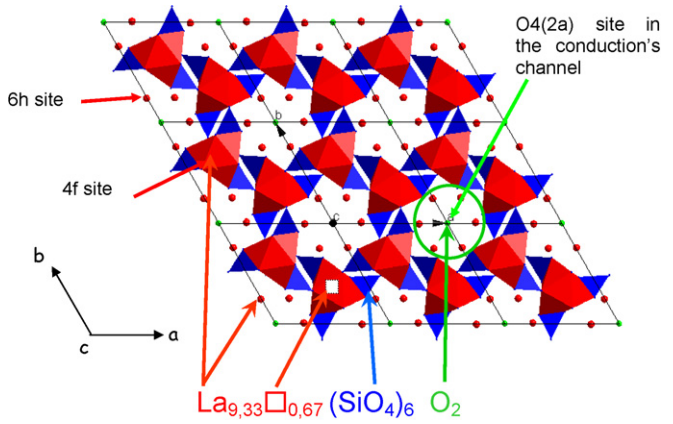

Fig. 1. *c*-Axis view of the crystal structure at room temperature of $La_{9.33}\square_{0.67}(SiO_4)_6O_2$ showing the SiO_4 groups as tetrahedra and La(4f), La(6h) and O(2a) atoms as balls.

Moreover, such processes are complex because they require a huge knowledge of all synthesis parameters otherwise they could lead to the formation of a great amount of secondary phases. In addition, these processes often produce nanocrystalline powders with a low conductivity.

In this study, we describe a new faster and lower temperature method for preparing pure apatite-type lanthanum silicate from a solid-state method. The high reactivity of the lanthanum oxide against H_2O and CO_2, transforming it into lanthanum hydroxide and carbonate, obviously influences its behaviour and the reactions with other compounds as reported by several authors.[13–22] The aging in ambient air involves a bulk hydroxylation and can also lead to a carbonation reaction. The carbonation process is suggested to occur mainly through the formation of surface carbonates or hydroxycarbonates. Additionally, when the number of carbonate groups increases, they become more and more difficult to remove with the temperature.[21] Such information must be taken into account to control the reactivity of La_2O_3 with SiO_2. The formation mechanism and the properties of the final products obtained from classical solid state reaction depend on the thermal history of the reagent powders.[15] Accordingly, we have studied the reaction of the starting mixture La_2O_3/SiO_2 (with La:Si = 9.33:6) during heating using X-ray diffraction (XRD), thermogravimetry coupled with differential thermal analysis (TG/DTA) and mass spectrometry (MS) in order to manage the formation of apatite. Especially, we propose a new method to avoid the formation of any secondary phase. Via this process, we have prepared and heated at different temperatures two compositions of apatite ($La_{9.33}(SiO_4)_6O_2$ and $La_{9.56}(SiO_4)_6O_{2.34}$). The structural and microstructural changes observed along the synthesis and sintering processes have been investigated using XRD and scanning electron microscopy (SEM). Ionic conductivity properties of the sintered materials have been measured and discussed.

2. Experimental

The apatite-type lanthanum silicates $La_{9.33+x}(SiO_4)_6O_{2+1.5x}$ ($x = 0$ and 0.23) were prepared by solid state reaction using high purity La_2O_3 (Aldrich, 99.9%) and SiO_2 (Prolabo, 99%) powders. La_2O_3 was previously dried at 800 °C for 30 min in order to eliminate lanthanum hydroxide and/or oxycarbonates and to determine the appropriate amount of this reagent. Oxides were first attrition milled for 3 h in ethanol at 450 rpm using a Union Process 01-Lab Attritor. Then, the ethanol was evaporated under vacuum at 45 °C. Different temperatures of calcination in the range 1200–1500 °C with a 4 h annealing time at each temperature, were tested in order to obtain these stoichiometric reactions:

$$(9.33/2)La_2O_3 + 6SiO_2 \rightarrow La_{9.33}(SiO_4)_6O_2 \quad (1)$$

$$(9.56/2)La_2O_3 + 6SiO_2 \rightarrow La_{9.56}(SiO_4)_6O_{2.34} \quad (2)$$

The calcined powders were uniaxially pressed (100 MPa) into pellets and then sintered in air at 1600 °C for 1 h resulting in disks with a diameter of ~10 mm and a thickness of ~2 mm. The densification of sintered materials was determined by geometrical measurements.

To investigate the La_2O_3/SiO_2 system, differential thermal analysis and thermogravimetry (DTA/TG) of the starting mixtures (with La:Si = 9.33:6) were performed using a TA Instruments SDT 2960 under helium atmosphere. The analysis of evolved gases was followed using a quadruple mass spectrometer (MS) (Pfeiffer vacuum thermostar) coupled together with the previous apparatus. The output of the mass spectrometer showed a plot of the relative intensity of a mass-to-charge ratio (noted *m/e* and corresponding to the molecular weight) versus the temperature.

Powders or pellets XRD patterns were recorded with a Siemens D5000 diffractometer (θ–2θ mode, Cu Kα radiation) in the 2θ range 20–60° (step size: 0.04°; time range: 45 min). The crystalline phases were identified using the International Centre for Diffraction Data (ICDD) Powder Diffraction Files (PDF).

The specific surface area of powders heated at different temperatures was measured using the Brunauer, Emmet and Teller (BET) method (eight points, N_2 gas analyzer Micromeritics ASAP 2010), after degassing under vacuum at 200 °C.

Microstructural investigations were made using SEM (Hitachi S2500). The surface of samples sintered at 1600 °C was prepared before observation by polishing with a SiC paper. Then, the microstructures were revealed by a thermal etching at 1550 °C for 30 min.

Ionic conductivity properties were measured by the complex impedance method using a Solartron 1260 Impedance/Gain Phase Analyzer. Measurements were made after coating opposite sides of sintered pellets with colloidal silver lac. The samples were characterized in the 250–600 °C temperature range, using frequencies from 1 Hz to 5 MHz.

3. Results and discussion

3.1. Thermal behaviour of La_2O_3/SiO_2 mixture

The mixture containing La_2O_3 (previously dried at 800 °C for 30 min) and SiO_2 (with La:Si = 9.33:6, Eq. (1)) was milled by attrition for 3 h in ethanol. In spite of such a care, La_2O_3

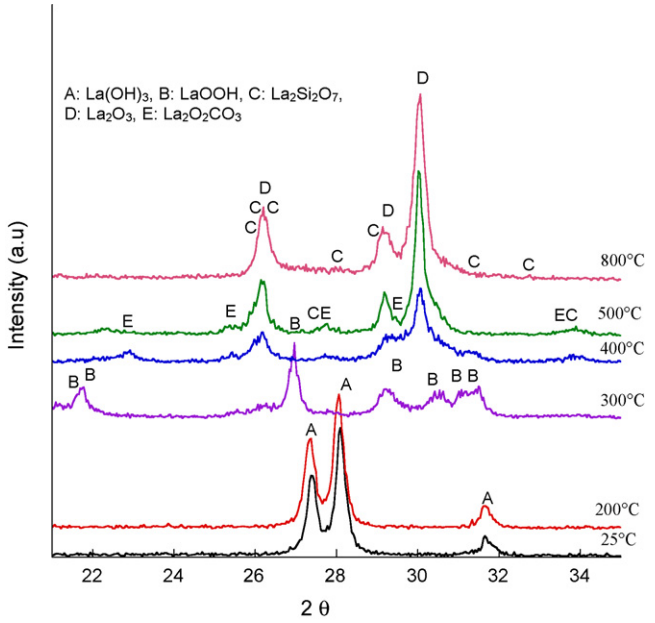

Fig. 2. XRD patterns of La_2O_3:SiO_2 (with La:Si = 9.33:6) sample prepared by the solid-state reaction technique after heat treatment at different temperatures.

was inevitably transformed into $La(OH)_3$ as detected on the XRD pattern (Fig. 2) at room temperature. As reported in the literature,[21] a carbonation process of the surface of $La(OH)_3$ could also occur in ethanol through the formation of hydroxycarbonates according to the following reactions.

$$La_2O_3 + 3H_2O \leftrightarrow 2La(OH)_3 \quad (3)$$

$$2La(OH)_3 + xCo_2 \leftrightarrow La_2(OH)_{6-2x}(CO_3)_x + xH_2O \quad (4)$$

The hydroxide phase could be surrounded by an highly disordered surface layer of hydroxycarbonate phases ($La_2(OH)_{6-2x}(CO_3)_x$; Eq. (4)), and the number of carbonated groups (x in Eq. (4)) would increase with the time of exposition to air.[23] XRD patterns (Fig. 2) showed the presence of different intermediate phases during heating which corresponded to the dehydration and decarbonation of lanthanum phases. In fact, $La(OH)_3$ or $La_2(OH)_{6-2x}(CO_3)_x$ compounds were thermally decomposed into LaOOH and $La_2O_2CO_3$ phases, both finally giving La_2O_3.

As deduced by TG and MS plots in Fig. 3(a and b), an experimental weight loss ($\Delta M/M_0$) of about 13.5 wt.% occurred during heating, which proceeded in three steps. The first two steps around 300 and 450 °C (noted I and II in Fig. 3) comprised the dehydration process of lanthanum hydroxide and hydroxycarbonate phases with H_2O releases at $m/e = 18$ (Fig. 3b) according to the following equilibrium reactions[14,15,24]:

$$2La(OH)_3 \overset{310^\circ C}{\longleftrightarrow} 2LaO(OH) + 2H_2O \quad (5)$$

$$2LaO(OH) \overset{460^\circ C}{\longleftrightarrow} La_2O_3 + H_2O \quad (6)$$

$$La_2(OH)_4(CO_3) \cdot nH_2O \overset{200^\circ C}{\longleftrightarrow} La_2(OH)_4(CO_3) + nH_2O \quad (7)$$

$$La_2(OH)_4(CO_3) \overset{430^\circ C}{\longleftrightarrow} La_2O_2(CO_3) + 2H_2O \quad (8)$$

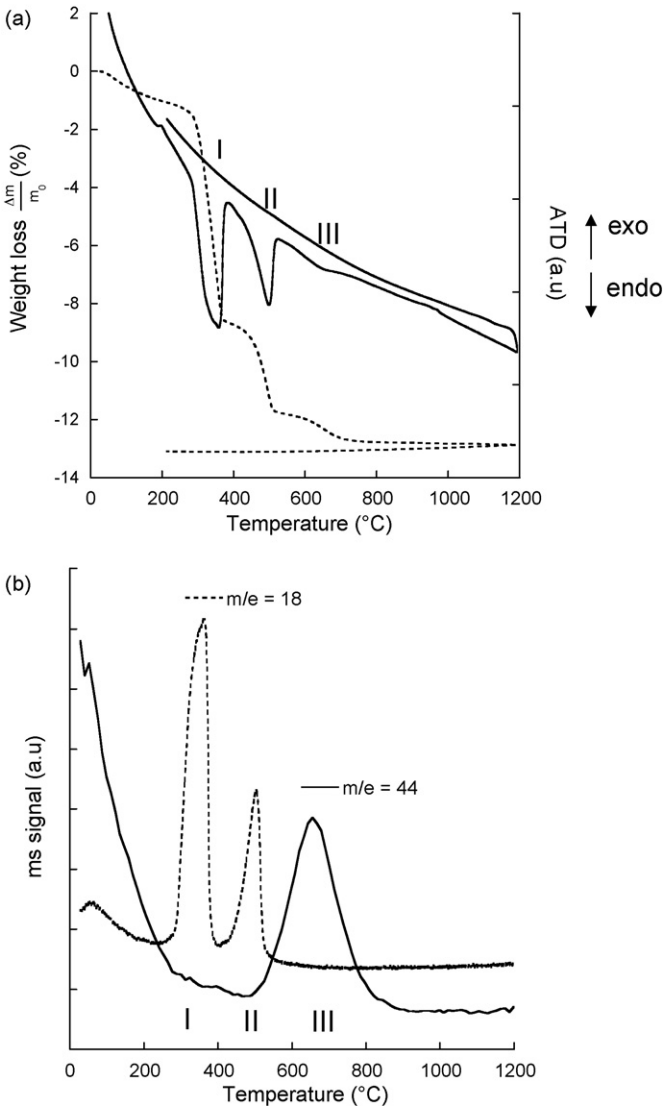

Fig. 3. (a) DTA-TG and (b) MS diagrams under helium atmosphere of the starting La_2O_3/SiO_2 (with La:Si = 9.33:6) mixture milled in ethanol.

The lanthanum hydroxide phase was totally dehydrated into La_2O_3 above 460 °C according to the reversible reactions (Eqs. (5) and (6)). The presence of the $La_2(OH)_{6-2x}(CO_3)_x$ phase at room temperature was also confirmed by DTA/TG analysis, Mass Spectrometry and by the detection on the XRD patterns, above 400 °C, of the $La_2O_2CO_3$ compound formed according to Eq. (8). Then, the third step corresponded to the decarbonation of this $La_2O_2CO_3$ intermediate phase, at about 650 °C, which was associated to a CO_2 gaseous release at $m/e = 44$ (Fig. 2b). It resulted in the formation of lanthanum oxide[21] according to:

$$La_2O_2CO_3 \overset{650^\circ C}{\longleftrightarrow} La_2O_3 + CO_2 \quad (9)$$

The La_2O_3 compound was completely formed only above 650 °C and could react with SiO_2 in order to produce an apatite phase according to the synthesis reactions listed in Eqs. (1) and (2). However, a secondary phase $La_2Si_2O_7$ was detected on the XRD pattern from 500 °C (Fig. 2). As reported on the phase equilibrium diagram of La_2O_3/SiO_2,[25] this phase is stable up

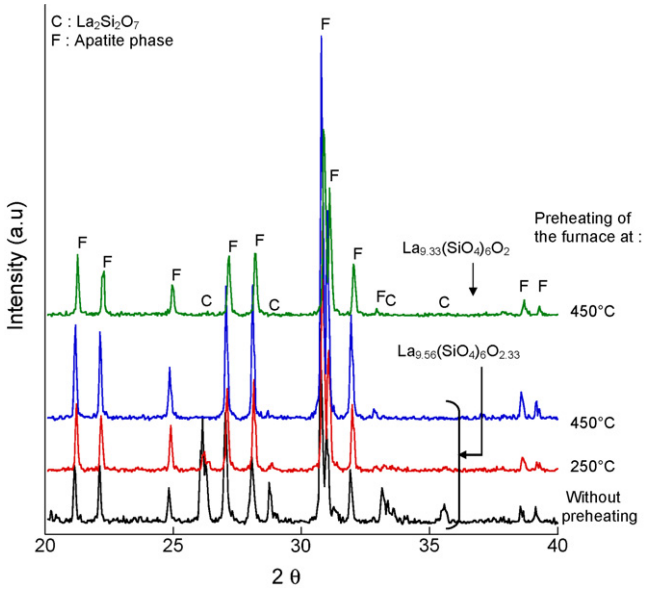

Fig. 4. Powder XRD patterns of mixtures calcined at 1500 °C for 4 h without or with preheating of the furnace at 250 and 450 °C.

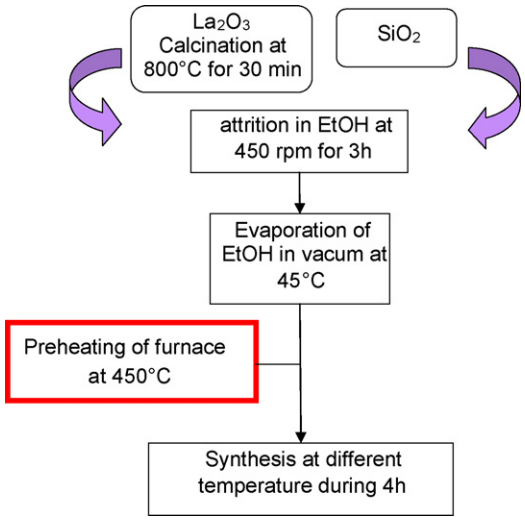

Fig. 5. Experimental procedure for the synthesis of pure apatite phases.

to 1750 °C and its elimination by sintering at high temperature appears difficult. It was still detected after calcination at 1500 °C for 3 h (see XRD pattern of the powder heated without preheating of the furnace in Fig. 4). The formation of this secondary phase was assumed to be related to the reaction between the intermediate LaO(OH) phase, formed after the decomposition of $La(OH)_3$ compound (Eq. (5)), and SiO_2 (Eq. (10)) as confirmed by XRD analysis. The reactivity of the intermediate phase LaO(OH) led it to react according to two competitive reactions (Eqs. (6) and (10)):

$$2LaO(OH) + 2SiO_2 \overset{\approx 450^\circ C}{\longleftrightarrow} La_2Si_2O_7 + H_2O \quad (10)$$

3.2. Synthesis and sintering

In order to eliminate the $La_2Si_2O_7$ impurity, it was necessary to use a suitable thermal treatment which can avoid the preliminary formation of the LaO(OH) compound. Therefore, two mixtures (with La:Si = 9.33:6 and 9.56:6, respectively) were attrition milled by attrition in ethanol and kept in a dry atmosphere at 130 °C to prevent hydration by atmospheric water vapour. A preheating of the furnace was also performed before the introduction of the powder mixture. A XRD study performed on the $La_{9.33}(SiO_4)_6O_2$ and $La_{9.56}(SiO_4)_6O_{2.33}$ compositions (Fig. 4) confirmed that this preheating before introducing the powder into the furnace had a direct influence on the purity of the final product after heating at 1500 °C for 4 h. In fact, a significant decrease of the intensity of the $La_2Si_2O_7$ phase diffraction peaks was observed for both $La_{9.33}(SiO_4)_6O_2$ (not shown) and $La_{9.56}(SiO_4)_6O_{2.33}$ (Fig. 4) samples when the furnace was preheated at 250 °C.

However, at this relatively low temperature, the dehydration of lanthanum hydroxide compounds was not total and so it did not lead to the formation of pure apatite. The formation of the $La_2Si_2O_7$ secondary phase was totally inhibited when the dry powders, kept at 130 °C, were placed into the furnace directly at 450 °C. The intermediate LaO(OH) phase was not formed above 460 °C and so the reaction written in Eq. (10) could not occur. This confirms the major role of this intermediate compound on the formation of the undesirable $La_2Si_2O_7$ phase. Consequently, pure powders of both $La_{9.33}(SiO_4)_6O_2$ and $La_{9.56}(SiO_4)_6O_{2.33}$ compositions could be synthesized using the experimental procedure summarized in Fig. 5.

The starting mixtures were first introduced in a furnace preheated at 450 °C and then calcined at different temperatures (1200, 1300, 1450 and 1500 °C) for 4 h in order to determine the temperature range allowing the preparation of a pure

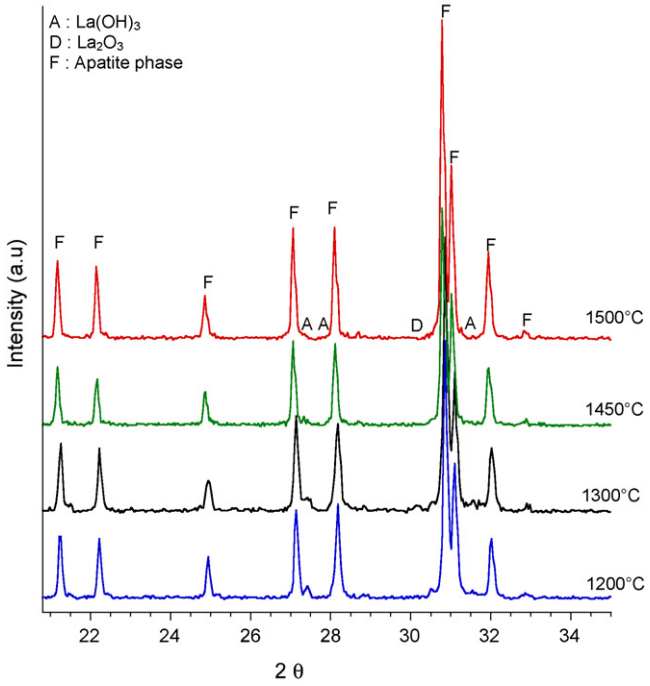

Fig. 6. XRD patterns of $La_{9.56}(SiO_4)_6O_{2.33}$ mixtures calcined at different temperatures (during 4 h) in a furnace previously preheated at 450 °C.

Table 1
Specific surface area of powders calcined at different temperatures

	Temperature of thermal treatment (during 4 h)				
	Starting mixture before calcination	1200 °C	1300 °C	1450 °C	1500 °C
Composition: $La_{9.33}(SiO_4)_6O_2$					
Specific surface area (m^2/g)	13.50	2.22	1.30	0.46	Not measurable
$La_{9.56}(SiO_4)_6O_{2.33}$					
Specific surface area (m^2/g)	13.50	2.13	1.31	0.80	Not measurable

apatite-type phase. The thermal behaviour of the hypothetical $La_{9.56}(SiO_4)_6O_{2.33}$ composition was investigated using XRD. It is shown in Fig. 6, and it is similar to that of $La_{9.33}(SiO_4)_6O_2$ compound. The final product is composed of an apatite-type lanthanum silicate phase without La_2SiO_5 or $La_2Si_2O_7$ secondary phase whatever the temperature might be.

So, well-crystallized and pure powders of lanthanum silicate oxyapatite can be obtained by a thermal treatment at a temperature as low as 1200 °C for only 4 h of annealing. This temperature is much lower than that of 1500 °C previously required by Vincent et al.[9] for the synthesis of oxyapatite compound using a classical high temperature solid-state reaction. This firing treatment is also much shorter than the 39 h at 1300 °C recommended by Leon-Reina et al.[4]

Moreover, this new fast- and low-temperature synthesis method that we have developed presents the advantage of limiting grain growth. Besides, thermal treatments at temperatures higher than 1450 °C of $La_{9.56}(SiO_4)_6O_{2.33}$ and $La_{9.33}(SiO_4)_6O_2$ powders have led to a decrease of their specific surface areas (Table 1). The formation of big agglomerates was confirmed on the SEM micrographs (Fig. 7). However, it must be noted that at this low synthesis temperatures some residual $La(OH)_3$ still remains after calcination (Fig. 6) indicating that the synthesis reaction (Eqs. (1) and (2)) was not complete.

Table 2
Densification ratio (%) of pellets sintered at 1600 °C during 1 h vs. the temperature of synthesis of the starting powders

	Temperature of powders synthesis during 4 h			
	1200 °C	1300 °C	1450 °C	1500 °C
Composition: $La_{9.33}(SiO_4)_6O_2$				
Densification ratio (%) after sintering at 1600 °C during 1 h	Broken	90.6	88.6	–
$La_{9.56}(SiO_4)_6O_{2.33}$				
Densification ratio (%) after sintering at 1600 °C during 1 h	92.6	90.2	75.7	70.0

The $La_{9.56}(SiO_4)_6O_{2.33}$ and $La_{9.33}(SiO_4)_6O_2$ powders synthesized at different temperature were pressed into pellets and then sintered at 1600 °C for 1 h. The final densification ratios are reported in Table 2 and show a strong decrease of the densification ratio (from 92.6 to 70.0%) of sintered pellets versus the temperature of synthesis. The reduction of densification ratios was linked to the large fall of the specific surface area (Table 1)

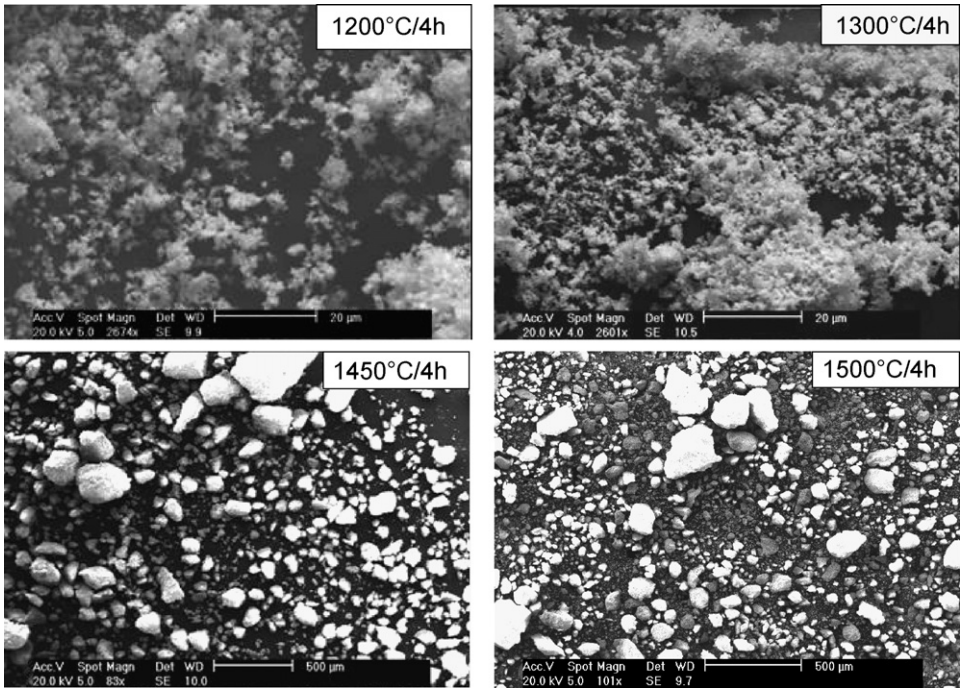

Fig. 7. SEM micrographs of $La_{9.56}(SiO_4)_6O_{2.33}$ samples calcined at different temperatures.

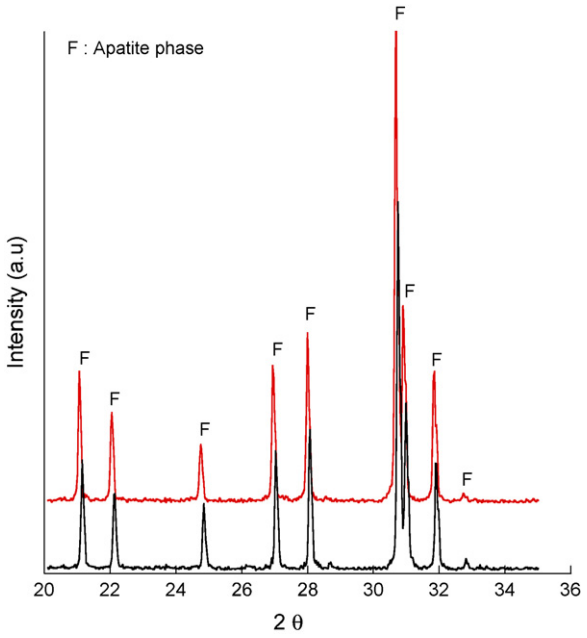

Fig. 8. XRD patterns of (a) $La_{9.33}(SiO_4)_6O_2$ and (b) $La_{9.56}(SiO_4)_6O_{2.33}$ pellets sintered at 1600 °C during 1 h from powders synthesized at 1300 °C during 4 h.

and the presence of hard agglomerates during the calcination at temperature which exceeding 1300 °C. So, the fast and low temperature ($T \leq 1300$ °C) synthesis method is essential to produce fine powders containing reactive particles, i.e. having a great surface area, in order to enhance the densification during the sintering.

The 1300 °C heat-treated powders made it possible to obtain pure and relatively dense pellets (≈90%) of $La_{9.33}(SiO_4)_6O_2$ and $La_{9.56}(SiO_4)_6O_{2.33}$ compositions after sintering at 1600 °C for 1 h (Fig. 8). Accordingly, this experimental procedure is an acceptable compromise for having a good purity of the pellet and a suitable densification ratio.

Nevertheless, the microstructure of dense pellets showed significant differences (Fig. 9) depending on the composition. The morphology of the starting powders was similar but the grain size after sintering was much bigger for $La_{9.33}(SiO_4)_6O_2$ than for $La_{9.56}(SiO_4)_6O_{2.33}$ compound (Fig. 9). The effect of oxygen and lanthanum additions modified the grain growth. Nevertheless, the surface of the sintered body did not show any particular sign of preferential orientation of grains during their growth, the relative intensity of the XRD peaks (Fig. 8) were comparable to that given by the PDF card.

3.3. Ionic conductivity of dense pellets

As the densification ratios were similar for $La_{9.33}(SiO_4)_6O_2$ and $La_{9.56}(SiO_4)_6O_{2.33}$ pellets after sintering at 1600 °C for 1 h from powders initially synthesised at 1300 °C for 4 h, it was possible to compare their bulk ionic conductivity versus the stoichiometry.

Fig. 10 shows the complex impedance plots obtained at 310 and 322 °C for $La_{9.33}(SiO_4)_6O_2$ and $La_{9.56}(SiO_4)_6O_{2.33}$ samples, respectively. These plots describe three semicircles: the

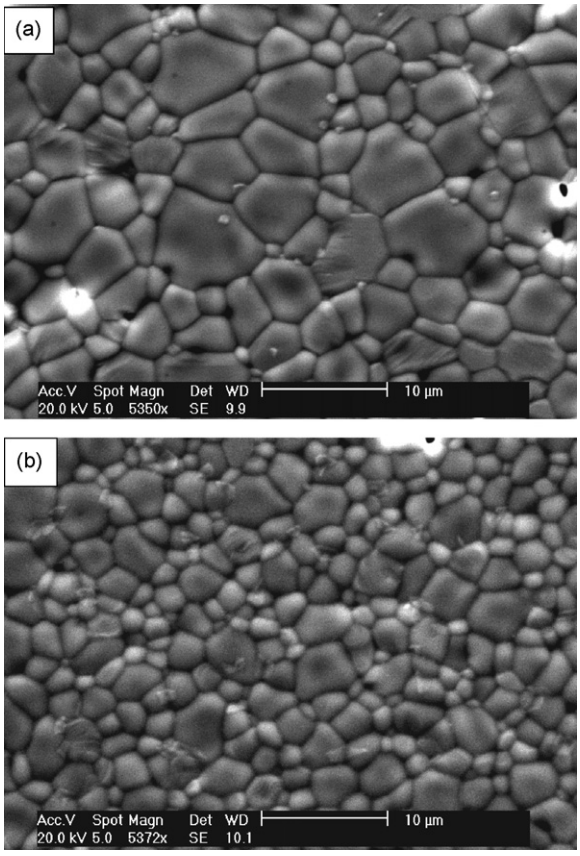

Fig. 9. SEM micrographs of the surface of (a) $La_{9.33}(SiO4)_6O_2$ and (b) $La_{9.56}(SiO_4)_6O_{2.33}$ pellets sintered at 1600 °C during 1 h from powders synthesized at 1300 °C during 4 h.

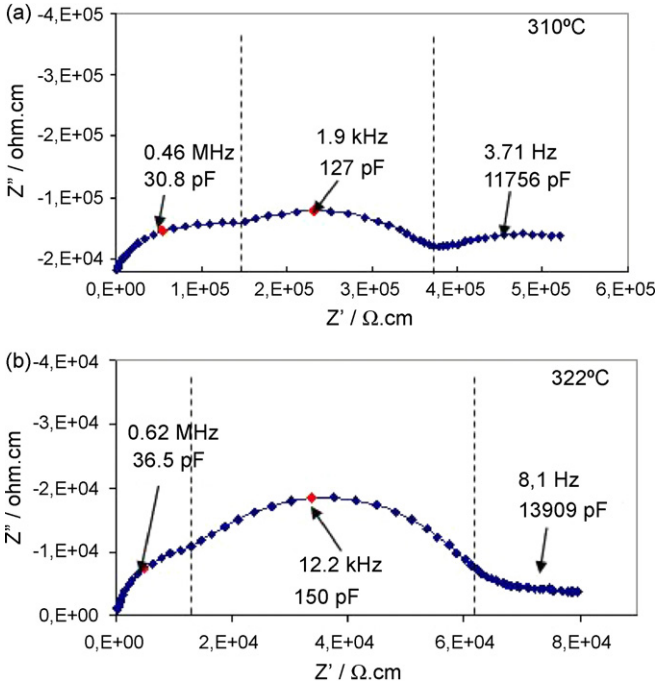

Fig. 10. Complex impedance plots of (a) $La_{9.33}(SiO_4)_6O_2$ and (b) $La_{9.56}(SiO_4)_6O_{2.33}$ compounds at 310 and 322 °C, respectively.

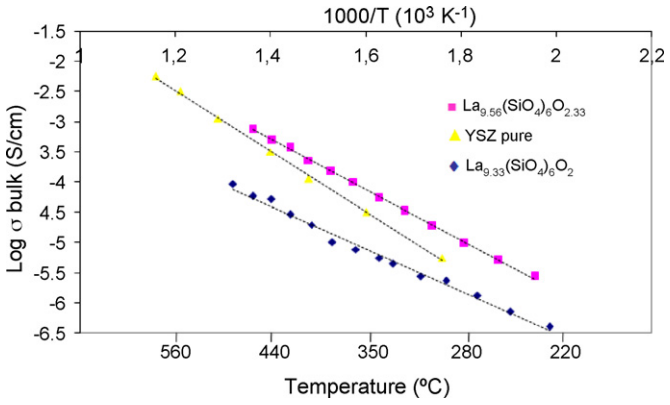

Fig. 11. Bulk ionic conductivity of $La_{9.33}(SiO_4)_6O_2$ and $La_{9.56}(SiO_4)_6O_{2.33}$ samples. Data on YSZ[1] are shown for comparison.

first one in the high-frequency region corresponds to the bulk response, whereas the second one, in the middle-frequency region, is related to the grain boundary contribution and the last one is due to the electrode interface contribution. It is worth noting that as the grain size of the two samples was different, this could induce some changes in the grain boundary response.

It was difficult to resolve bulk and grain boundary semicircles for both compositions (Fig. 10) since the conductivity of these samples was high ($\sigma_{bulk} = 1.5 \times 10^{-4}$ S cm^{-1} and 1.4×10^{-3} S cm^{-1} at 500 °C for $La_{9.33}(SiO_4)_6O_2$ and $La_{9.56}(SiO_4)_6O_{2.33}$ phases respectively). Moreover, these samples had a measurable conductivity at temperature as low as 200 °C. The activation energy was low (0.7 and 0.8 eV, respectively) and the bulk conductivity of $La_{9.56}(SiO_4)_6O_{2.33}$ material was ten times higher than that of $La_{9.33}(SiO_4)_6O_2$ compound.

A possible explanation for the higher ionic conductivity of $La_{9.56}(SiO_4)_6O_{2.33}$ sample is that the composition had an excess of oxide ions. As observed by Yoshioka,[5] the incorporation of extra oxide ions with increasing the La content from $x = 9.33$ to 9.92 enhances the ionic conductivity. We have compared our results with their result, though care must be taken because discrepancy can arise from the measurements methods and from the refinement of the complex impedance plots, and we have found that our $La_{9.56}(SiO_4)_6O_{2.33}$ material exhibits a bulk conductivity which was double the $La_{9.6}(SiO_4)_6O_{2.4}$ compound ($\sigma_{bulk} = 0.6 \times 10^{-3}$ S cm^{-1} at 500 °C).

Fig. 11 shows bulk ionic conductivities (in a typical Arrhenius-type plot) of our apatite materials and of pure yttria stabilized zirconia (YSZ).[1] $La_{9.56}(SiO_4)_6O_{2.33}$ composition presents a higher bulk ionic conductivity than traditional YSZ electrolyte in this temperature range (200–500 °C). Such material could become very attractive as an ionic conductor[8,26] for SOFC device.

4. Conclusion

We have developed a new fast and low-temperature method to synthesize pure $La_{9.33+x}(SiO_4)_6O_{2+1.5x}$ lanthanum silicate oxyapatite materials. The formation of $La_2Si_2O_7$ secondary phase, which forms by a chemical reaction between LaO(OH) and SiO_2, can be completely eliminated by keeping La_2O_3 reactant in dry atmosphere and putting the powder mixture into a furnace preheated at 450 °C. Using this process, the formation of the LaO(OH) intermediate phase was avoided and pure $La_{9.33}(SiO_4)_6O_2$ and $La_{9.56}(SiO_4)_6O_{2.33}$ apatite phases were synthesized at a much lower temperature (1200 °C) than that used in conventional powder solid-state synthesis routes (typically 1500–1600 °C). Thus, more reactive particles were obtained after calcination which enhanced the densification after further sintering. Moreover, the hypothetical compositions like $La_{9.33+x}(SiO_4)_6O_{2+1.5x}$ ($x > 0$) were corroborated by the fabrication of these two different materials with characteristic properties. The limit $La_{10}(SiO_4)_6O_3$ composition is actively investigated and some authors[7,8,11] reported that this phase would exist but such a composition remains suspicious and is obtained with a great amount of secondary phases.[5]

We have shown that the bulk conductivity of the sintered $La_{9.56}(SiO_4)_6O_{2.33}$ body was much higher at 500 °C, than that of $La_{9.33}(SiO_4)_6O_2$ sample and than traditional YSZ oxide ion conductors. Accordingly, we confirmed that the existence of oxide ions excess into the structure has an important role for high ionic conductivity. Moreover, this conductivity may improve the more, the more that the oxide ion excess accepted by $La_{9.33+x}(SiO_4)_6O_{2+1.5x}$ structure can be increased ($x > 0.27$).

Further investigations will be the direct use of these pure oxyapatite powders synthesized at low temperature, in plasma spraying or tape casting processes in order to manufacture a SOFC. The investigation of the oxide-ion conduction mechanisms using the bond valence method and defect energy calculations in lanthanum silicate oxyapatite phase is also in progress.

References

1. Marques, F. M. B., Kharton, V. V., Naumovich, E. N., Shaula, A. L., Kovalevsky, A. V. and Yaremchenko, A. A., Oxygen ion conductors for fuel cells and membranes: selected developments. *Solid State Ionics*, 2006, **177**, 1697–1703.
2. Masubuchi, Y., Higuchi, M., Takeda, T. and Kikkawa, S., Preparation of apatite-type $La_{9.33}(SiO_4)_6O_2$ oxide ion conductor by alcoxide-hydrolysis. *J. Alloys Compd.*, 2006, **408–412**, 641–644.
3. Yoshioka, H. and Tanase, S., Magnesium doped lanthanum silicate with apatite-type structure as an electrolyte for intermediate temperature solid oxide fuel cells. *Solid State Ionics*, 2005, **176**, 2395–2398.
4. Leon-Reina, L., Losilla, E. R., Martinez-Lara, M., Bruque, S. and Aranda, M. A. G., Interstitial oxygen conduction in lanthanum oxy-apatite electrolytes. *J. Mater. Chem.*, 2004, **14**, 1142–1149.
5. Yoshioka, H., Oxide ionic conductivity of apatite-type lanthanum silicates. *J. Alloys Compd.*, 2006, **408–412**, 649–652.
6. Lambert, S., Vincent, A., Bruneton, E., Beaudet-Savignat, S., Guillet, F., Minot, B. and Bouree, F., Structural investigation of $La_{9.33}Si_6O_{26}$- and $La_9AESi_6O_{26+\delta}$-doped apatites-type lanthanum silicate (AE=Ba, Sr and Ca) by neutron powder diffraction. *J. Solid State Chem.*, 2006, **179**, 2602–2608.
7. Nakayama, S., Aono, H. and Sadaoka, Y., Ionic conductivity of $Ln_{10}(SiO_4)_6O_3$ (Ln=La, Nd, Sm, Gd and Dy). *Chem. Lett.*, 1995, 431–432.
8. Nakayama, S. and Sakamoto, M., Electrical properties of new type high oxide ionic conductor $RE_{10}Si_6O_{27}$ (RE=La, Pr, Nd, Sm, Gd, Dy). *J. Eur. Ceram. Soc.*, 1998, **18**, 1413–1418.
9. Vincent, A., Savignat, S. B. and Gervais, F., Elaboration and ionic conduction of apatite-type lanthanum silicates doped with Ba, $La_{10-x}Ba_x(SiO_4)_6O_{3-x/2}$ with x=0.25–2. *J. Eur. Ceram. Soc.*, 2007, **27**, 1187–1192.

10. Celerier, S., Laberty-Robert, C., Ansart, F., Calmet, C. and Stevens, P., Synthesis by sol–gel route of oxyapatite powders for dense ceramics: applications as electrolytes for solid oxide fuel cells. *J. Eur. Ceram. Soc.*, 2005, **25**, 2665–2668.
11. Tao, S. and Irvine, J. T. S., Preparation and characterisation of apatite-type lanthanum silicates by a sol–gel process. *Mater. Res. Bull.*, 2001, **36**, 1245–1258.
12. Fuentes, A. F., Rodriguez-Reyna, E., Martínez-González, L. G., Maczka, M., Hanuza, J. and Amador, U., Room-temperature synthesis of apatite-type lanthanum silicates by mechanically milling constituent oxides. *Solid State Ionics*, 2006, **177**, 1869–1873.
13. Bernal, S., Botana, F. J., Garcia, R. and Rodriguez-Izquierdo, J. M., Thermal evolution of a sample of La_2O_3 exposed to the atmosphere. *Thermochim. Acta*, 1983, **66**, 139–145.
14. Bernal, S., Diaz, J. A., Garcia, R. and Rodriguez-Izquierdo, J. M., Study of some aspects of the reactivity of La_2O_3 with CO_2 and H_2O. *J. Mater. Sci.*, 1985, **20**, 537–541.
15. Bernal, S., Botana, F. J., Garcia, R., Ramirez, F. and Rodriguez-Izquierdo, J. M., Solid state chemistry of the preparation of lanthana-supported metal catalysts-study of the impregnation step. *J. Mater. Sci.*, 1987, **22**, 3793–3800.
16. Bernal, S., Blanco, G., Delgado, J. J., Finol, D., Gatica, J. M., Rodriguez-Izquierdo, J. M. and Vidal, H., Investigation by means of H_2 adsorption, diffraction, and electron microscopy techniques of a cerium/terbium mixed oxide supported on a lanthana-modified alumina. *Chem. Mater.*, 2002, **14**, 844–850.
17. Bernal, S., Blanco, G., Calvino, J. J., Omil, J. A. P. and Pintado, J. M., Some major aspects of the chemical behavior of rare earth oxides: An overview. *J. Alloys Compd.*, 2006, **408–412**, 496–502.
18. Toops, T. J., Walters, A. B. and Vannice, M. A., The effect of CO_2, H_2O and SO_2 on the kinetics of NO reduction by CH_4 over La_2O_3. *Appl. Catal. B: Environ.*, 2002, **38**, 183–199.
19. Vidal, H., Bernal, S., Baker, R. T., Finol, D., Omil, J. A. P., Pintado, J. M. and Rodriguez-Izquierdo, J. M., Characterization of La_2O_3/SiO_2 mixed oxide catalyst supports. *J. Catal.*, 1999, **183**, 53–62.
20. Vidal, H., Bernal, S., Baker, R. T., Cifredo, G. A., Finol, D. and Rodriguez-Izquierdo, J. M., Catalytic behavior of lanthana promoted Rh/SiO_2 catalysts: influence of the preparation procedure. *Appl. Catal. A*, 2001, **208**, 111–123.
21. Bernal, S., Blanco, G., Gatica, J. A., Omil, J. A. P., Pintado, J. M. and Vidal, H., In *Chemical reactivity of binary rare earth oxides in binary rare earth oxides*, ed. G. A. Adachi, N. Imanaka and Z. Zang. Kluwer Academic Plenum Press, London, 2004, pp. 9–55.
22. Belous, A., Yanchevskiy, O. and V'yunov, O., Peculiarities of $Li_{0.5}La_{0.5}TiO_3$ formation during the synthesis by solid-state reaction or precipitation from solutions. *Chem. Mater.*, 2004, **16**, 407–417.
23. Rodulfo-Baechler, S. M. A., Pernia, W., Aray, I., Figueroa, H. and Gonzalez-Cortes, S. L., Influence of lanthanum carbonate phases of $Ni/La_{0.98}Sr_{0.02}O_x$ catalyst over the oxidative transformation of methane. *Catal. Lett.*, 2006, **112**, 231–237.
24. Tzvetkov, G. and Minkova, N., Application of mechanochemical treatment to the synthesis of A- and G-forms of $La_2Si_2O_7$. *Solid State Ionics*, 1999, **116**, 241–248.
25. Toropov, N. A., *Izv. Akad. Nauk. SSSR, Ser. Khim.*, 1962, 1365.
26. Arikawa, H., Nishiguchi, H., Ishihara, T. and Takita, Y., Oxide ion conductivity in Sr-doped $La_{10}Ge_6O_{27}$ apatite oxide. *Solid State Ionics*, 2000, **136/137**, 31–37.